

PAPER • OPEN ACCESS

## Aspects of Shape Coexistence in the Geometric Collective Model of Nuclei

To cite this article: P. E. Georgoudis and A. Leviatan 2018 *J. Phys.: Conf. Ser.* **966** 012043

View the [article online](#) for updates and enhancements.

### Related content

- [Shape coexistence and evolution in neutron-deficient krypton isotopes](#)  
Bai Zhi-Jun, Fu Xi-Ming, Jiao Chang-Feng et al.
- [Theoretical Study on the Rotational Bands and Shape Coexistence of  \$^{179,181,183}\text{Au}\$  in the Particle-Triaxial-Rotor Model](#)  
Chen Guo-Jie, Liu Yu-Xin and Song Hui-Chao
- [Prolate and Oblate Shape Coexistence in  \$^{188}\text{Pt}\$](#)   
Liu Yuan, Zhou Xiao-Hong, Zhang Yu-Hu et al.

# Aspects of Shape Coexistence in the Geometric Collective Model of Nuclei

**P. E. Georgoudis and A. Leviatan**

Racah Institute of Physics, The Hebrew University, 91904, Jerusalem, Israel

E-mail: panos@phys.huji.ac.il, ami@phys.huji.ac.il

**Abstract.** We examine the coexistence of spherical and  $\gamma$ -unstable deformed nuclear shapes, described by an  $SO(5)$ -invariant Bohr Hamiltonian, along the critical-line. Calculations are performed in the Algebraic Collective Model by introducing two separate bases, optimized to accommodate simultaneously different forms of dynamics. We demonstrate the need to modify the  $\beta$ -dependence of the moments of inertia, in order to obtain an adequate description of such shape-coexistence.

## 1. Introduction

The Geometric Collective Model (GCM) [1] plays a central role in the study of nuclear shapes and, more recently, in providing a convenient framework for incorporating beyond mean-field effects, essential for understanding phase transitions between such shapes. Of particular current experimental and theoretical interest, are first-order transitions involving coexistence of distinct shapes in the same nucleus. In the present contribution, we examine such coexistence of spherical and  $\gamma$ -unstable deformed shapes in the vicinity of the critical-line. In this case, the relevant Bohr Hamiltonian involves a  $\gamma$ -independent potential, supporting two degenerate minima. We employ an algebraic formulation of the GCM, the Algebraic Collective Model (ACM) [2, 3], which makes exact numerical calculations feasible, without recourse to approximations such as  $\beta$ -rigidity and adiabaticity, hence can reveal general capabilities and limitations of the GCM.

## 2. The Geometric Collective Model with $SO(5)$ symmetry

The Bohr Hamiltonian in the quadrupole variables reads

$$\hat{H} = -\frac{\hbar^2}{2B} \left( \frac{1}{\beta^4} \frac{\partial}{\partial \beta} \beta^4 \frac{\partial}{\partial \beta} - \frac{\hat{\Lambda}^2}{\beta^2} \right) + V(\beta, \gamma). \quad (1)$$

Here  $B$  is a mass parameter and  $\hat{\Lambda}^2 = -\frac{1}{\sin 3\gamma} \frac{\partial}{\partial \gamma} \sin 3\gamma \frac{\partial}{\partial \gamma} + \frac{1}{4} \sum_k \frac{L_k^2}{\sin^2(\gamma - \frac{2}{3}\pi k)}$  is the Casimir operator of  $SO(5)$ , acting on the  $\gamma$  and three Euler angles  $\Omega$ . When the potential depends only on  $\beta$ ,  $V(\beta, \gamma) \mapsto V(\beta)$ , the Hamiltonian has  $SO(5)$  symmetry and the wave functions can be separated into two parts,  $\Psi(\beta, \gamma, \Omega) = f(\beta) \mathcal{Y}_{\tau n_{\Delta} LM}(\gamma, \Omega)$ , satisfying the following equations

$$\hat{\Lambda}^2 \mathcal{Y}_{\tau n_{\Delta} LM}(\gamma, \Omega) = \tau(\tau + 3) \mathcal{Y}_{\tau n_{\Delta} LM}(\gamma, \Omega), \quad (2a)$$

$$\left[ -\frac{1}{\beta^4} \frac{\partial}{\partial \beta} \beta^4 \frac{\partial}{\partial \beta} + \frac{\tau(\tau + 3)}{\beta^2} + v(\beta) \right] f(\beta) = \epsilon f(\beta). \quad (2b)$$



Here  $\epsilon = \frac{2B}{\hbar^2}E$  and  $v(\beta) = \frac{2B}{\hbar^2}V(\beta)$  are the reduced energy and potential, respectively.  $\mathcal{Y}_{\tau, n_\Delta, L, M}$  are  $SO(5)$  basis states with good  $SO(5) \supset SO(3)$  quantum numbers  $(\tau, L)$ , and  $n_\Delta$  a multiplicity label. By setting  $\phi(\beta) = \beta^2 f(\beta)$ , Eq. (2b) can be cast in the form of a radial Schrödinger equation

$$-\frac{d^2\phi}{d\beta^2} + \left[ \frac{(\tau+1)(\tau+2)}{\beta^2} + v(\beta) \right] \phi = \epsilon \phi. \quad (3)$$

with an effective  $\tau$ -dependent potential

$$v_{eff}^{(\tau)}(\beta) = \frac{(\tau+1)(\tau+2)}{\beta^2} + v(\beta). \quad (4)$$

The ACM provides a tractable algebraic scheme for an exact numerical diagonalization of the Bohr Hamiltonian (1), in a basis of  $SU(1,1) \times SO(5)$  product wave functions,  $R_\nu^\lambda(a\beta)\mathcal{Y}_{\tau n_\Delta LM}(\gamma, \Omega)$ . The angular part are the  $SO(5)$  spherical harmonics of Eq. (2a), and the radial part are  $SU(1,1)$  modified oscillator wave functions given by [2, 3]

$$R_\nu^\lambda(a\beta) = (-1)^\nu \sqrt{\frac{2\nu!a}{\Gamma(\nu+\lambda)}} (a\beta)^{\lambda-1/2} e^{-a^2\beta^2/2} L_\nu^{(\lambda-1)}(a^2\beta^2) \quad \nu = 0, 1, 2, \dots \quad (5)$$

where  $L_\nu^{(\lambda-1)}$  is a generalized Laguerre polynomial of order  $\nu$ . Any choice of  $\lambda > 0$  defines an orthonormal  $SU(1,1)$  basis, in which matrix elements of the potential can be evaluated in closed form. For  $\lambda = \tau + 5/2$ , the above set reduces to the spherical harmonic oscillator basis. In general, the scaling parameter  $a$  and  $\lambda$  affect the width and localization of  $R_\nu^\lambda(a\beta)$ , respectively. An optimal choice of  $(a, \lambda)$ , enables a faster convergence as a function of basis size. For  $\gamma$ -independent potentials, with even powers of  $\beta$ , this implies that converged results can be obtained with only a few basis states (small  $\nu_{max}$ ) in the expansion of the radial wave function

$$\phi(\beta; a, \lambda) = \sum_{\nu=0}^{\nu_{max}} c_\nu^{(\tau)} R_\nu^\lambda(a\beta), \quad (6)$$

where the expansion coefficients,  $c_\nu^{(\tau)}$ , depend on  $\tau$ . The ACM has so far been tested for potentials with a single minimum [2, 3]. In the present work, we extend this approach to accommodate potentials  $v(\beta)$  with multiple minima.

### 3. Shape coexistence in the GCM with $\gamma$ -independent potentials

The dynamics associated with  $\gamma$ -independent potentials with a single minimum, has been studied extensively. For a single minimum at  $\beta = 0$ , the spectrum resembles that of a spherical vibrator, describing quadrupole excitations of a spherical shape. The levels are arranged in  $n_d$ -multiplets composed of states with quantum numbers  $(n_d = 0, \tau = 0, L = 0)$ ,  $(n_d = 1, \tau = 1, L = 2)$ ,  $(n_d = 2, \tau = 0, L = 0; \tau = 2, L = 2, 4)$  and  $(n_d = 3, \tau = 3, L = 0, 3, 4, 6; \tau = 1, L = 2)$ , in increasing order. For a single minimum at  $\beta > 0$ , the spectrum resembles that of a  $\gamma$ -unstable deformed roto-vibrator, with  $\beta$  excitations of the deformed equilibrium shape. The ground band is composed of  $\tau$ -multiplets with quantum numbers  $(\tau = 0, L = 0)$ ,  $(\tau = 1, L = 2)$ ,  $(\tau = 2, L = 2, 4)$  and  $(\tau = 3, L = 0, 3, 4, 6)$ , in increasing order. The same pattern repeats itself in excited  $\beta$ -bands. The dynamics at the critical-point of a second-order shape-phase transition, where the spherical minimum evolves continuously into a deformed minimum, can be modeled by a flat-bottomed potential. Analytic benchmarks for these three limits of structure are the harmonic spherical vibrator model [4] (similar to the  $U(5)$  dynamical symmetry of the interacting boson model (IBM) [5]), the  $\beta$ -rigid Jean-Wilets model [4] (similar to the  $SO(6)$  dynamical symmetry of the IBM), and the  $E(5)$  critical-point model [6] (an infinite square-well potential), respectively. Characteristic signatures for these solvable limits are listed in Table 1.

**Table 1.** Characteristic properties of yrast states for GCM paradigms: a spherical vibrator [4], E(5) critical-point [6] and  $\gamma$ -unstable deformed rotor [4]. B(E2) values are in units of  $B(E2; 2_1^+ \rightarrow 0_1^+) = 100$ . The E2 operator is proportional to the quadrupole coordinate  $\alpha_{2\mu}$ .

Observable	Spherical vibrator [U(5)]	E(5)	$\gamma$ -unstable deformed rotor [SO(6)]
$E(4_1^+)/E(2_1^+)$	2	2.20	2.5
$E(6_1^+)/E(2_1^+)$	3	3.59	4.5
$B(E2; 4_1^+ \rightarrow 2_1^+)$	200	168	143
$B(E2; 6_1^+ \rightarrow 4_1^+)$	300	221	167

In the present work, we explore the dynamics of shape coexistence in the GCM, with an SO(5)-invariant Bohr Hamiltonian. We focus the discussion to the critical-line of a first-order phase transition involving the coexistence of spherical and  $\gamma$ -unstable deformed shapes. This can be modeled by the following sextic potential in the Bohr Hamiltonian

$$v(\beta) = v_0 \beta^2 (\beta^2 - \beta_0^2)^2, \quad (7)$$

where  $v_0 = \frac{2B}{\hbar^2} V_0$  is the reduced strength.  $v(\beta)$  is an even function of  $\beta$  and is independent of  $\gamma$ , ensuring an SO(5) symmetry for the Hamiltonian. For  $v_0 > 0$ , it supports two degenerate global minima, spherical ( $\beta = 0$ ) and deformed ( $\beta = \beta_0 > 0$ ), at zero energy. A local maximum at  $\beta = \frac{1}{\sqrt{3}}\beta_0$  creates a barrier of height  $B_h = \frac{4}{27}v_0\beta_0^6$ , separating the two minima. The two wells are asymmetric with different stiffness,  $v''(\beta = \beta_0) = 4v''(\beta = 0) = 8v_0\beta_0^4$ . The barrier-height and potential stiffness are related, both increasing linearly with  $v_0$  and as a power-law with  $\beta_0$ . The spherical well is finite, while the deformed well has a finite interior boundary and an exterior wall rising as  $\beta^6$  for  $\beta \rightarrow \infty$ . Both wells become wider for higher energy.

Finite-N aspects of the dynamics in such potentials have been studied [7] in the framework of the IBM, based on a compact U(6) spectrum generating algebra. Here we examine the analogous dynamics in the GCM, which has an inherent non-compact algebraic structure. The sextic potential in question, does not belong to a class of solvable nor quasi-solvable potentials, hence the radial equation (3) necessitates a numerical solution. For that purpose, we employ the ACM approach. To facilitate the identification and convergence of different types of states, we diagonalize the Bohr Hamiltonian with  $v(\beta)$ , Eq. (7), in two different  $SU(1, 1) \times SO(5)$  bases

$$\Psi_s = \beta^{-2} \phi_s(\beta; a_s, \lambda_s) \mathcal{Y}_{\tau n_\Delta LM}(\gamma, \Omega), \quad (8a)$$

$$\Psi_d = \beta^{-2} \phi_d(\beta; a_d, \lambda_d) \mathcal{Y}_{\tau n_\Delta LM}(\gamma, \Omega). \quad (8b)$$

Here the radial wave functions are defined as in Eq. (6), and are characterized by different parameters  $(a_s, \lambda_s) \neq (a_d, \lambda_d)$ . In particular, the basis  $\Psi_s$  of Eq. (8a) [ $\Psi_d$  of Eq. (8b)] is appropriate for spherical [deformed] type of states, associated with the spherical [deformed] minimum, and consequently,  $\lambda_s \ll \lambda_d$ . The convergence is verified by examining the energies, B(E2) values and orthogonality of the calculated states,  $\Psi_s$  and  $\Psi_d$ .

#### 4. Evolution of structure along the critical-line

The spectrum and eigenstates of the Bohr Hamiltonian is governed by the competition between the potential and kinetic-rotational terms. The potential term is attractive and tends to localize the wave functions in the vicinity of its minima. In general, “deepening” a potential lowers the energies of levels confined within it, while “narrowing” a potential raises the level energies. The

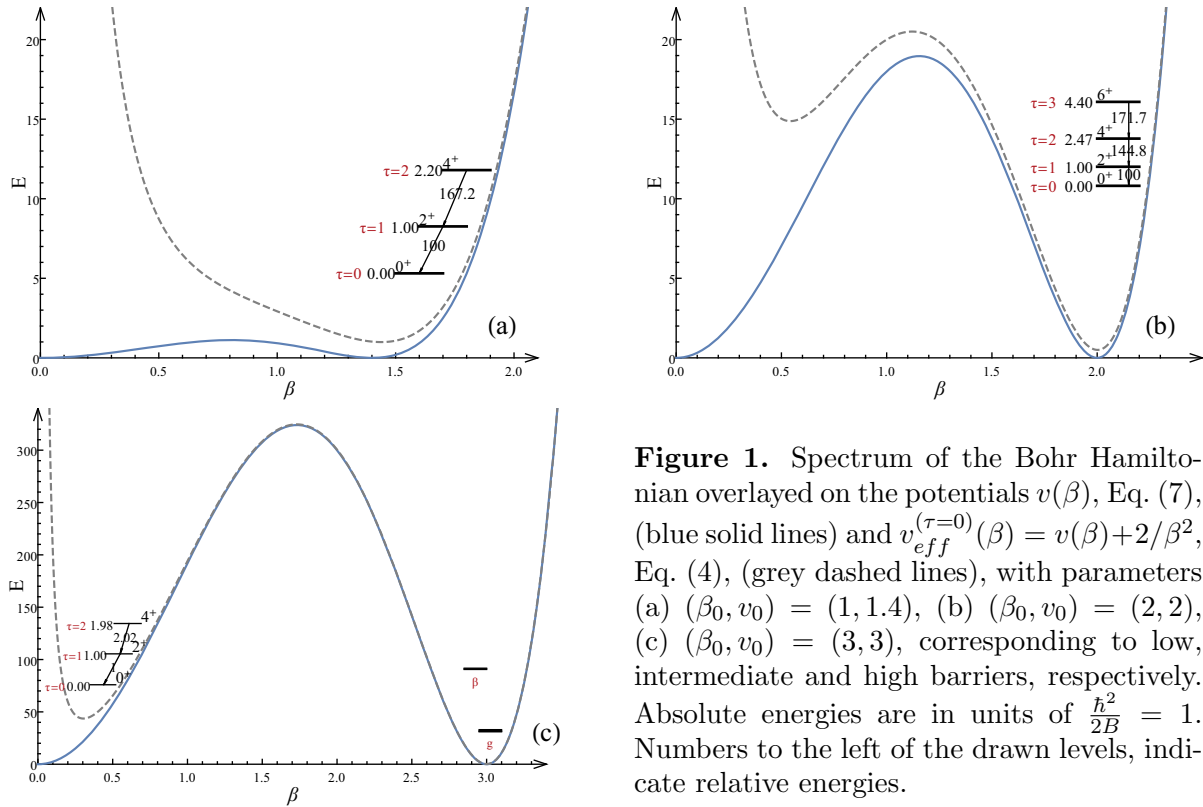


**Figure 1.** Spectrum of the Bohr Hamiltonian overlaid on the potentials  $v(\beta)$ , Eq. (7), (blue solid lines) and  $v_{eff}^{(\tau=0)}(\beta) = v(\beta) + 2/\beta^2$ , Eq. (4), (grey dashed lines), with parameters (a)  $(\beta_0, v_0) = (1, 1.4)$ , (b)  $(\beta_0, v_0) = (2, 2)$ , (c)  $(\beta_0, v_0) = (3, 3)$ , corresponding to low, intermediate and high barriers, respectively. Absolute energies are in units of  $\frac{\hbar^2}{2B} = 1$ . Numbers to the left of the drawn levels, indicate relative energies.

kinetic term,  $\frac{1}{\beta^2} \hat{\Lambda}^2$ , is repulsive and tends to delocalize the wave-functions. Its strength depends on  $\tau$  and the  $1/\beta^2$  dependence energetically penalizes small  $\beta$  values and tends to “push” the wave function towards larger  $\beta$ . This affects strongly the spherical minimum in the effective potential  $v_{eff}^{(\tau)}(\beta)$ , Eq. (4), shifting its position to larger values of  $\beta$  and distorting its shape. In contrast, the kinetic term has a marginal effect on the shape of the deformed well, yet it governs the rotational splitting of states in the associated ground and excited bands. These effects are seen clearly in Fig. 1, displaying the energy spectrum overlaid on the potentials  $v(\beta)$  and  $v_{eff}^{(\tau=0)}(\beta)$ , for representative values of  $(v_0, \beta_0)$ . Fig. 1(a) corresponds to the case of a low-barrier. The energy levels are well above the barrier and experience essentially a flat bottomed potential. The spectrum resembles that of the E(5) critical-point model (see Table 1 for comparison). Higher levels show the spectral character of a  $\beta^6$  potential. The kinetic term present in the effective potential, completely washes out the spherical minimum. Fig. 1(b) corresponds to the case of an intermediate-barrier. Here a spherical minimum develops in  $v_{eff}^{(\tau=0)}(\beta)$  but is shifted to higher energy and is distorted by the kinetic term to such an extent, that it does not support bound states. The spectrum consists only of deformed type of states, forming a ground band with and SO(6)-like structure. Fig. 1(c) corresponds to the case of a high barrier. Here both the spherical and deformed minima are well developed and support bound states localized in their vicinity. The deformed states comprise the ground and  $\beta$  bands. Their rotational splitting, shown in Fig. 2, exhibits an SO(6)-like character. The spherical states are arranged in  $n_d$ -multiplets and exhibit a U(5)-like structure.

## 5. Limitation of the standard GCM Hamiltonian and a possible resolution

Figs. 1(c)-2, demonstrate a limitation of the standard GCM Hamiltonian, namely, very different energy scales for the rotational and vibrational excitations. A pronounced coexistence of many

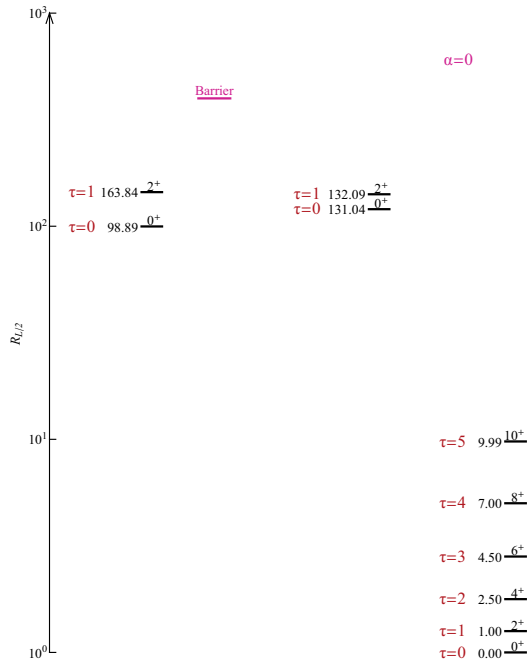


**Figure 2.** Selected levels in the ground band (right),  $\beta$ -band (middle) and spherical states (left) for the Bohr Hamiltonian with  $(\beta_0, v_0, \alpha) = (3, 3, 0)$ . Energies are in units of  $R_{L/2} = \frac{E(L) - E(0_1^+)}{E(2_1^+) - E(0_1^+)}$ .

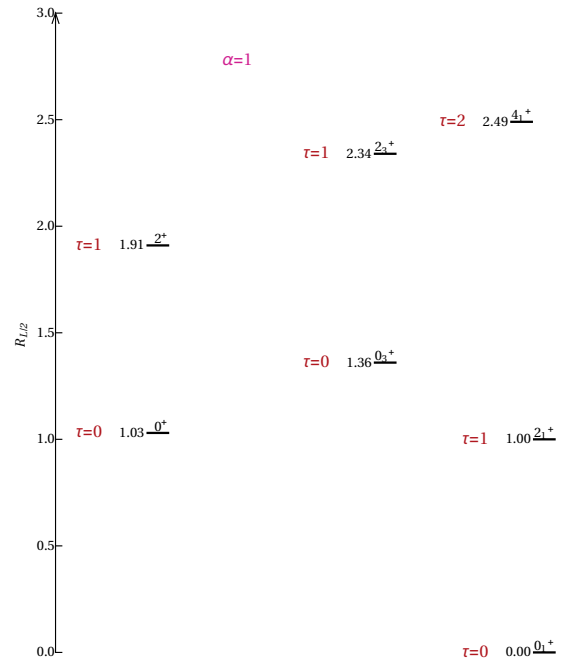


**Figure 3.** As in Fig. 2, but for a Bohr Hamiltonian with  $(\beta_0, v_0, \alpha) = (3, 3, 1)$  in Eqs. (7) and (9). Note the linear energy scale as opposed to the logarithmic energy scale in Fig. 2.

spherical and deformed states requires the two wells to be deep with a high-barrier in-between. For the potential under study, this necessitates a large deformation  $\beta_0$ . The states localized within the deformed potential have an average deformation  $\langle \beta^2 \rangle$  of order  $\beta_0^2$ , increasing with  $\tau$ , hence experience a small rotational splitting of order  $\tau(\tau + 3)/\beta_0^2$ , with noticeable centrifugal stretching. For the same  $\beta_0$ , the stiffness of the deformed minimum is large, hence the  $\beta$ -bandhead energy is high, of order  $\epsilon_\beta \approx 4\beta_0^2 v_0$ . The kinetic term shifts the position of the spherical minimum to a small but non-zero value of  $\beta$ , hence the lowest spherical  $0_s^+$  state experiences a shift of order  $2/\langle \beta^2 \rangle$  to higher energy. For the example considered in Figs. 1(c) and 2,  $E(2_1^+) - E(0_1^+) = 0.45$ , while  $\frac{E(0_\beta^+) - E(0_1^+)}{E(2_1^+) - E(0_1^+)} = 131.06$  and  $\frac{E(0_s^+) - E(0_1^+)}{E(2_1^+) - E(0_1^+)} = 98.90$ , *i.e.*, the resulting rotational and vibrational scales differ by more than two-orders of magnitude. Such a difference is at variance with the experimentally observed patterns of coexistence in nuclei.

The origin of the problem can be traced to the quadratic  $\beta$ -dependence of the irrotational moments of inertia in the kinetic term,  $\frac{1}{\beta^2} \hat{\Lambda}^2$ . A possible resolution is to allow a departure from such a  $\beta^2$  behavior. In the present study, we consider the following substitution

$$\frac{1}{\beta^2} \hat{\Lambda}^2 \rightarrow \frac{(1 + \alpha\beta^2)^2}{\beta^2} \hat{\Lambda}^2. \quad (9)$$

This particular choice is motivated by previous studies within the GCM [8, 9] and the classical limit of the IBM [10]. For  $\alpha \neq 0$ , this introduces an additional term,  $\alpha(2 + \alpha\beta^2)\tau(\tau + 3)$ , in the radial equation, which affects only the levels with  $\tau \neq 0$ . Typical spectrum and E2 decay pattern, obtained with  $\alpha = 1$ , are shown in Figs. 3-4. Many states now occur below the barrier, with

6.89 Barrier

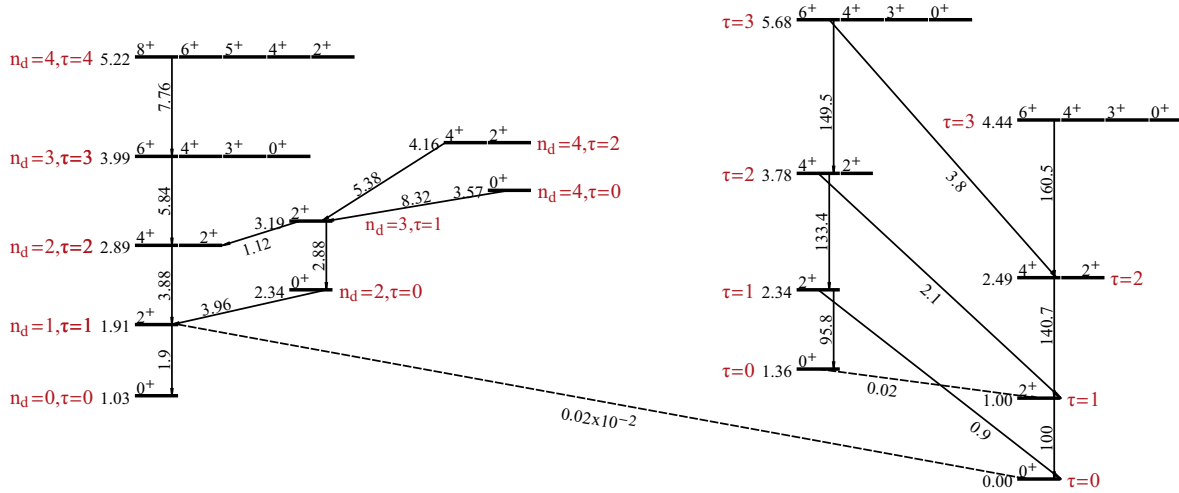


**Figure 4.** Spectrum of the Bohr Hamiltonian with  $(\beta_0, v_0, \alpha) = (3, 3, 1)$  in Eqs. (7) and (9). Converged results for spherical (left side) and deformed (right side) type of states, are obtained by employing  $SU(1, 1) \times SO(5)$  bases, Eq. (8), with  $(a_s, \lambda_s) = (4, 2.5)$  and  $(a_d, \lambda_d) = (4.1, 140.5)$ , respectively.  $L = 0_1^+, 0_3^+$  are the bandhead states of the ground and  $\beta$  bands, with  $\sqrt{\langle \beta^2 \rangle} = 2.97, 2.93$ , respectively.  $L = 0_2^+$  is the spherical ground state with  $\sqrt{\langle \beta^2 \rangle} = 0.41$ .

comparable rotational and vibrational scales. The spherical states exhibit a  $U(5)$ -like structure, with strong  $\Delta n_d = \pm 1$  E2 decays. The deformed states (comprising the ground and  $\beta$ -bands) maintain an  $SO(6)$ -like structure, with strong (weak) intra-band (inter-band) transitions. The E2 decays between the spherical and deformed type of states are extremely weak, reflecting the impact of the high barrier. The ability of a single Hamiltonian to accommodate simultaneously states with different symmetry character, reinforces the view that partial symmetries can play a role in the phenomena of shape coexistence [7, 11, 12].

### Acknowledgments

This work is supported by the Israel Science Foundation Grant No. 586/16. P.E.G. acknowledges the Golda Meir Fellowship Fund for partial support. We thank M.A. Caprio for assistance in using his ACM numerical code.

### References

- [1] Bohr A and Mottelson B R 1975 *Nuclear Structure* (MA: Benjamin Reading)
- [2] Rowe D J and Turner P S 2005 *Nucl. Phys. A* **753** 94
- [3] Rowe D J, Welsh T A and Caprio M A 2009 *Phys. Rev. C* **79** 054304
- [4] Rowe D J and Wood J L 2010 *Fundamentals of Nuclear Models* (Singapore: World Scientific)
- [5] Iachello F and Arima A 1987 *The Interacting Boson Model* (Cambridge: Cambridge University Press)
- [6] Iachello F 2000, *Phys. Rev. Lett.* **85** 3580
- [7] Leviatan A and Gavrielov N 2017 *Phys. Scr.* **92** 114005
- [8] Bonatsos D, Georgoudis P E, Lenis D, Minkov N and Quesne C 2011 *Phys. Rev. C* **83** 044321
- [9] Georgoudis P E 2014 *Phys. Lett. B* **731** 122
- [10] Bonatsos D, Minkov N and Petrellis D 2015 *J. Phys. G* **42** 095104
- [11] Leviatan A 2007 *Phys. Rev. Lett.* **98** 242502
- [12] Leviatan A and Shapira D 2016 *Phys. Rev. C* **93** 051302(R)